

## Transient Step Bunching on a Vicinal Si(111) Surface

H. Hibino and T. Ogino

*NTT Basic Research Laboratories, Atsugi, Kanagawa 243-01, Japan*

(Received 21 June 1993)

We used high-temperature scanning tunneling microscopy to observe, in real time, the step rearrangement induced by a  $(7\times 7)$  reconstructive phase transition on a vicinal Si(111) surface misoriented toward  $[\bar{1}\bar{1}2]$ . A new transient step bunching is found between a high-temperature phase consisting of single-layer steps with nonreconstructed terraces and a low-temperature phase of a mixture of single- and triple-layer steps with  $(7\times 7)$  reconstructed terraces. The transient step bunching indicates that the free energy of the  $(7\times 7)$  reconstructed step edge is larger than that of the nonreconstructed step edge just below the phase transition temperature.

PACS numbers: 61.16.Ch, 68.35.Bs, 68.35.Md, 68.35.Rh

Step arrangements on vicinal surfaces have received much interest, primarily because vicinal surfaces have been used for basic studies of epitaxial growth mechanisms [1] and for the fabrication of such sophisticated structures as fractional-order superlattices [2]. The stability of the vicinal surface has been widely explained by the Wulff plot, which enables the equilibrium crystal shape to be determined from the orientational dependence of the surface energy [3]. It is difficult, however, to obtain the orientational dependence of the surface energy experimentally. The total free energy of the vicinal surface is determined by the surface free energy of terraces, the individual step free energy, and the step interaction energy. In discussing the stability of the vicinal surface, it is important to estimate these values. The free energies on vicinal semiconductor surfaces are strongly dependent on reconstructions, which are usually formed on the terraces to reduce the number of dangling bonds. Reconstructive phase transitions therefore sometimes induce step rearrangements. Vicinal Si(111) surfaces, for example, are uniformly covered with single-layer steps (each 3.14 Å high) above the  $(1\times 1)\leftrightarrow(7\times 7)$  phase transition temperature ( $T_c$ ). The step arrangement below  $T_c$ , however, depends on the misorientation direction: On a surface misoriented toward  $[1\bar{1}0]$  or  $[11\bar{2}]$ ,  $T_c$  decreases with increasing misorientation angle and the surface is separated into  $(7\times 7)$  reconstructed (111) facets and step bunches [4,5]; and on a surface misoriented toward  $[\bar{1}\bar{1}2]$ ,  $T_c$  is independent of the misorientation angle and the surface is covered with single- and triple-layer steps [6,7].

If we are to understand the step arrangements on vicinal Si(111) surfaces, real-space and real-time observations of the step rearrangement during the phase transition between  $(1\times 1)$  and  $(7\times 7)$  structures are essential. Recent low-energy electron microscopy (LEEM) studies have revealed a new phenomenon occurring as the (111) facet forms on vicinal Si(111) surfaces misoriented toward  $[11\bar{2}]$  [8]. That is, the (111) facet has a saturation width determined by strain relaxation. We and our co-workers have also investigated (111) facet formation by using high-temperature scanning tunneling microscopy

(HT-STM), whose higher spatial resolution revealed a critical terrace width for the  $(1\times 1)\rightarrow(7\times 7)$  phase transition and that terrace width changes in units of  $(7\times 7)$  reconstruction [9,10]. In this paper, we present the results of using HT-STM to observe step rearrangement on a vicinal Si(111) surface misoriented toward  $[\bar{1}\bar{1}2]$ . A new transient step bunching is demonstrated and interpreted in simple energetics of the vicinal surface. *This transient step bunching confirms a general principle of surface thermodynamics pointed out by Bartelt, Einstein, and Rottman [11]. That is, a first-order phase transition between surfaces with different step structures proceeds through a step bunched phase.* We also describe the pathway in the formation of a triple-layer step that explains the correlation of the  $(7\times 7)$  reconstruction across a single-layer step [12].

Vicinal Si(111) samples (B doped,  $\rho=1-10\ \Omega\text{cm}$ ) were misoriented  $1.8^\circ$  toward the  $[\bar{1}\bar{1}2]$  direction. After a sample was chemically cleaned by repeated oxidation in  $\text{H}_2\text{O}_2:\text{H}_2\text{SO}_4$  (1:4) and oxide removal in HF solution, it was degassed under ultrahigh vacuum at about  $50^\circ\text{C}$  for 3–10 h. After degassing, the sample was flashed at  $1250^\circ\text{C}$  several times. Before HT-STM measurement, the sample was kept at the test temperature for about an hour. The base pressure of the STM chamber was  $2\times 10^{-10}$  torr and was kept below  $1\times 10^{-9}$  torr while the sample was annealed by passing a dc current through it. This annealing current flow was in the step-down direction ( $[\bar{1}\bar{1}2]$  direction) because current flowing in the step-up direction causes continuous growth of the  $(7\times 7)$ -reconstructed terraces observed in HT-STM images and ultrahigh-vacuum scanning-electron-microscopy (UHV-SEM) images [13]. The sample temperature was measured by an infrared pyrometer. HT-STM images were taken in both constant-height and constant-current modes. The sample bias during annealing was estimated under the assumption that the voltage for sample annealing dropped uniformly across the sample and the STM tip approached at the middle of the sample. Typical values for sample bias and tunneling current were 2 V and 0.2 nA.

We first investigated the motion of individual steps.

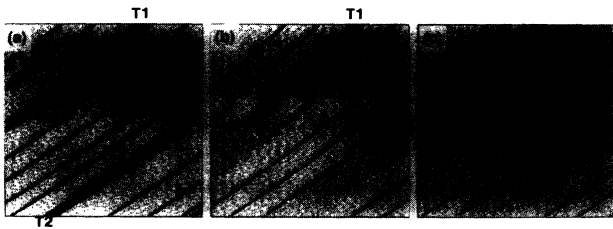


FIG. 1. Constant-height STM images of a vicinal Si(111) surface misoriented  $1.8^\circ$  toward  $[\bar{1}\bar{1}2]$ . Sample temperatures are (a)  $820^\circ\text{C}$ , (b) during heating, and (c)  $823^\circ\text{C}$ . (Scanning area:  $900\times 900 \text{ \AA}$ . Sample bias: 2 V. Tunneling current: 0.2 nA.)

Figures 1(a)–1(c) show constant-height STM images taken at temperatures between  $820$  and  $823^\circ\text{C}$ . The sample temperature was increased while taking the image shown in Fig. 1(b), causing the drift seen in the image. Figure 1(a) shows both single-layer and triple-layer steps. All the terraces seen in Fig. 1(a) have  $(7\times 7)$  reconstruction and are quantized by a  $(7\times 7)$  unit cell. The  $(7\times 7)$  reconstruction is shifted by a defined vector across the single-layer step [12]. The step edges are very straight and stable except for occasional sudden changes in terrace width, such as the one marked *A* in Fig. 1(a). *This is because the  $(7\times 7)$  reconstructed step edge directed toward  $[\bar{1}\bar{1}2]$  is energetically more favorable than those directed in other directions [14].* Figure 1 also shows that the width changes, too, are quantized by a  $(7\times 7)$  unit cell. After the temperature was increased, on the other hand, fuzzy steps and rough regions around them were observed. Figure 1(b) shows that this is due to the separation of the triple-layer steps (*T1* and *T2*) into three single-layer steps. *This separation occurs because the energy cost for forming a triple-layer step from three single-layer steps is balanced with the energy loss due to the reduction of the  $(7\times 7)$ -reconstructed area.* Although Fig. 1(b) shows that the  $(7\times 7) \rightarrow (1\times 1)$  phase transitions occurs on the terraces (*W1* and *W2*) adjacent to the triple-layer step, the separation of the triple-layer step is not usually accompanied by such  $(7\times 7) \rightarrow (1\times 1)$  phase transitions. During the formation and destruction of triple-layer steps, we sometimes observed a pair consisting of a single-layer step and a double-layer step such as that marked *T1* in Fig. 1(a), and the single-layer step was always the uppermost of the three steps. A periodic array of double-layer steps is observed on the long-annealed surface [15] and the As-adsorbed surface [16]. Double-layer steps are probably energetically metastable.

We also investigated the temperature dependence of the step arrangement, and Fig. 2 shows constant-current STM images taken while increasing the sample temperature from  $820$  to  $830^\circ\text{C}$ . The thermal drift during this heating was so small that a specific terrace (indicated by an arrow) can be traced. The surface shown in Fig. 2(a) is covered with single-layer and triple-layer steps. The  $(7\times 7)$  reconstruction is on all the terraces of this surface,

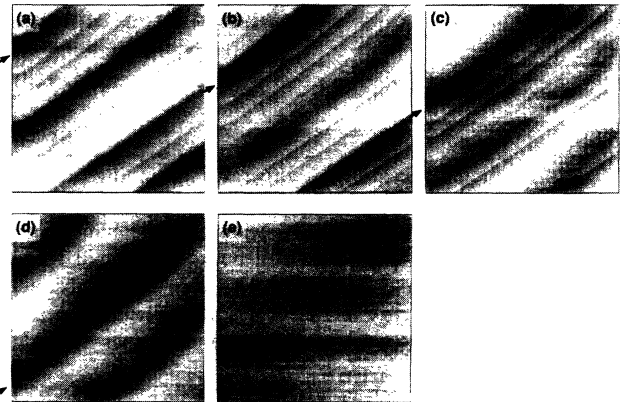


FIG. 2. Constant-current STM images of a vicinal Si(111) surface misoriented  $1.8^\circ$  toward  $[\bar{1}\bar{1}2]$ . Sample temperatures are (a)  $820^\circ\text{C}$ , (b)  $824^\circ\text{C}$ , (c)  $825^\circ\text{C}$ , (d)  $828^\circ\text{C}$ , and (e)  $830^\circ\text{C}$ . (Scanning area:  $1000\times 100 \text{ \AA}$ . Sample bias: 2 V. Tunneling current: 0.2 nA.)

but atomic images of the  $(7\times 7)$  reconstruction cannot be seen because of the limited number of pixel points. The triple-layer steps seen in Figs. 2(b) and 2(c), like those shown in Fig. 1, are separated. In these figures, we can see that the steps between two  $(7\times 7)$ -reconstructed terraces are straight and stable, but that the steps between  $(7\times 7)$ -reconstructed and -nonreconstructed terraces are fuzzy and unstable. As shown in Fig. 2(d), step bunching occurs when the temperature is further increased. The step rearrangement that took place when the temperature was increased from  $825$  to  $828^\circ\text{C}$  occurred in a very peculiar manner, as will be discussed in more detail in the following paragraph. Because the step bunches are stable between the critical temperature for the step bunching ( $T_b$ ) and  $T_c$ , they are not a transition state but are an equilibrium condition. We also used UHV-SEM to ob-

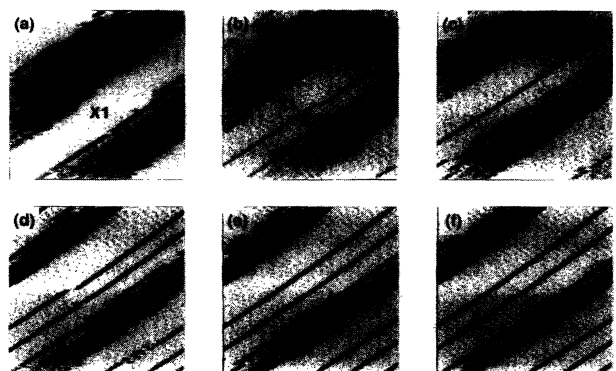


FIG. 3. Constant-height STM images taken while the sample temperature was decreased near  $825^\circ\text{C}$ . The images shown in (a)–(f) were taken at times 0, 35, 87.5, 122.5, 157.5, and 175 s. (Scanning area:  $750\times 750 \text{ \AA}$ . Sample bias: 2 V. Tunneling current: 0.2 nA.)

serve step bunching on a sample annealed by an ac current, and this means that step bunching is not induced by a dc current [13,17]. As shown in Fig. 2(e), when the surface temperature was increased above  $T_c$ , step bunches disappear at the same time that the  $(7 \times 7)$  reconstruction disappears, leaving the surface uniformly covered with single-layer steps. The step rearrangement during cooling was almost exactly the opposite of that during heating.

The step rearrangement *between the step bunched surface and the reconstructed stepped surface covered with single- and triple-layer steps* is shown in detail in the STM images in Fig. 3. Figure 3(a) shows the step bunching. In Fig. 3(b), however, the  $(1 \times 1) \rightarrow (7 \times 7)$  phase transition occurs on a side terrace  $X_2$  lower than the  $(7 \times 7)$ -reconstructed terrace. The step  $S_1$  between the  $(7 \times 7)$ -reconstructed terraces ( $X_1$  and  $X_2$ ) moves to equalize these terrace widths. This terrace width equalization is due to repulsive step interaction. The  $(1 \times 1) \rightarrow (7 \times 7)$  phase transition usually occurred on the lower side terrace, but we sometimes also observed it on the higher side terrace. This  $(7 \times 7)$  formation on the lower side terrace and terrace width equalization, which was not perfect, occurred repeatedly until three steps were left between the  $(7 \times 7)$ -reconstructed terraces. *The STM images in Fig. 3 were taken during cooling. Figure 3 therefore probably proves that the step rearrangement is not completed at a phase transition temperature but in a certain temperature range. All terraces are reconstructed below  $T_i$ , and between  $T_b$  and  $T_i$  the step bunched surface and the reconstructed stepped surface are gradually transformed into each other. The step rearrangement during the  $(1 \times 1) \leftrightarrow (7 \times 7)$  transition is summarized in Fig. 4. This step rearrangement is in good agreement with the case shown in Fig. 2(b) in Ref. [18].*

Consider a vicinal surface on which the step interaction energy is proportional to  $1/l^2$ ,  $l$  being the average terrace width. When the step density on this surface is uniform, the total surface free energy per unit area is expressed as

$$f^{\text{uni}}(n, T) = f^0(T) + \beta(T)n + \phi(T)n^3,$$

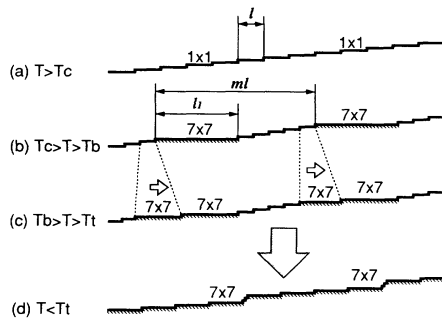


FIG. 4. Schematic views of the temperature dependent step arrangement on a vicinal Si(111) surface misoriented  $1.8^\circ$  toward  $[112]$ .

where  $n$  is  $1/l$ ,  $f^0(T)$  is the surface energy of the terrace,  $\beta(T)$  is the individual step free energy, and  $\phi(T)n^3$  corresponds to the step interaction energy. The terms  $f^0(T)$ ,  $\beta(T)$ , and  $\phi(T)$  depend on the reconstruction, but in the following discussions,  $\phi(T)$  is assumed to be independent of the reconstruction:  $\phi_{(1 \times 1)}(T) = \phi_{(7 \times 7)}(T)$ . Moreover, triple-layer step formation is ignored because on  $1.3^\circ$ - and  $2.7^\circ$ -misoriented surfaces there are far fewer triple-layer steps than single-layer steps [19] and above  $T_i$  there are no triple-layer steps. *In reality, the coexistence of single- and triple-layer steps below  $T_i$  indicates that the difference between their step free energies per step is very small [20]. We therefore ignore the triple-layer step in the following discussions.* From the definition of  $T_c$ , we know that  $f_{(1 \times 1)}^0(T) < f_{(7 \times 7)}^0(T)$  at  $T > T_c$  and that  $f_{(1 \times 1)}^0(T) > f_{(7 \times 7)}^0(T)$  at  $T < T_c$ . Because the  $(1 \times 1) \leftrightarrow (7 \times 7)$  phase transition is a first-order phase transition [21], it is reasonable to think that  $\beta_{(1 \times 1)}(T) < \beta_{(7 \times 7)}(T)$  near  $T_c$ . Moreover, as will be shown later, the occurrence of transient step bunching is well explained by  $\beta_{(1 \times 1)}(T) < \beta_{(7 \times 7)}(T)$ . At  $T > T_c$ ,  $f_{(1 \times 1)}^0(T) < f_{(7 \times 7)}^0(T)$  and  $\beta_{(1 \times 1)}(T) < \beta_{(7 \times 7)}(T)$ , resulting in the surface consisting of nonreconstructed terraces and single-layer steps. At  $T < T_c$ ,  $f_{(1 \times 1)}^0(T) > f_{(7 \times 7)}^0(T)$  but  $\beta_{(1 \times 1)}(T) < \beta_{(7 \times 7)}(T)$ . *Using the construction of the tie lines between  $f_{(1 \times 1)}^{\text{uni}}$  and  $f_{(7 \times 7)}^{\text{uni}}$ , we can understand the step configuration change [11,20]. Above  $T_b$ , the tie line is tangential to  $f_{(1 \times 1)}^{\text{uni}}$  but intersects with  $f_{(7 \times 7)}^{\text{uni}}$  at  $n=0$  when steps are bunched. Between  $T_b$  and  $T_i$ , the tie line is tangential to both  $f_{(1 \times 1)}^{\text{uni}}$  and  $f_{(7 \times 7)}^{\text{uni}}$ , and the step density of the vicinal surface is between the two tangential points. This means the nonreconstructed step bunched phase coexists with the reconstructed stepped phase.*

The terms  $f^0(T)$  and  $\beta(T)$  can be estimated using our experimental results and the reported  $\phi(T)$  value [7,20,22]. The relation between  $f_{(1 \times 1)}^0(T) - f_{(7 \times 7)}^0(T)$  and  $\phi(T)$  is obtained from a condition minimizing the total free energy  $f^{\text{sb}}$  of the vicinal surface on which steps are bunched. Consider a periodic arrangement of a  $(7 \times 7)$ -reconstructed terrace  $l_1$  wide and  $(m-1)$  nonreconstructed terraces as shown in Fig. 4(b). Then  $f^{\text{sb}}$  is expressed as

$$mf^{\text{sb}} = (ml - l_1)f_{(1 \times 1)}^0 + l_1f_{(7 \times 7)}^0 + (m-2)\beta_{(1 \times 1)} + \beta_{(7 \times 7)}^{\text{up}} + \beta_{(7 \times 7)}^{\text{down}} + \phi/l_1^2 + \phi(m-1)^3/(ml - l_1)^2,$$

where  $\beta_{(7 \times 7)}^{\text{up}}$  and  $\beta_{(7 \times 7)}^{\text{down}}$  are the free energies of the steps that have a  $(7 \times 7)$ -reconstructed terrace on the lower and higher side.  $\beta_{(7 \times 7)}^{\text{up}}$  and  $\beta_{(7 \times 7)}^{\text{down}}$  are not equal to  $\beta_{(7 \times 7)}$ . The minimization condition,  $df^{\text{sb}}/dl_1 = 0$ , gives  $\Delta f^0 = f_{(1 \times 1)}^0 - f_{(7 \times 7)}^0 = 2\phi(m-1)^3/(ml - l_1)^3 - 2\phi/l_1^3$ . Substituting  $m$  and  $l_1$  values measured in STM images taken at  $828^\circ\text{C}$  [Fig. 2(d)], we have  $\Delta f^0(T) = (4.6 \times 10^{-6}) \times \phi(T)$ . The reported  $\phi$  value of  $450 \text{ meV } \text{\AA}$  [20,22] gives  $\Delta f^0(T) = 2.1 \times 10^{-3} \text{ meV } \text{\AA}^{-2}$ . If we assume that  $\Delta f^0(T) = [\Delta f^0(T=0 \text{ K})](T_c - T)/T_c$ , then  $\Delta f^0(T=0$

$K) = 1.1 \text{ meV}/\text{\AA}^2$ . This value is less than  $\Delta f^0(T=0 \text{ K}) = 60 \text{ meV}/(1 \times 1) \text{ unit cell} = 4.7 \text{ meV}/\text{\AA}^2$ , which corresponds to the energy difference between  $(2 \times 2)$  and  $(7 \times 7)$  reconstructions [23,24], and  $\Delta f^0(T=0 \text{ K}) = 4.5 \text{ meV}/\text{\AA}^2$ , which is determined experimentally [20]. One possible reason for this difference is that the step-down dc current keeps the  $(7 \times 7)$ -reconstructed terrace narrower than those annealed by ac currents [25] and the quantity  $\Delta f^0$  is therefore underestimated. The quantity  $\beta_{(7 \times 7)} \times (T_t) - \beta_{(1 \times 1)}(T_t)$  can be estimated from the condition that the tie line is tangential to  $f_{(7 \times 7)}^{\text{uni}}$  at  $n=0.1$ . This relation gives  $\beta_{(7 \times 7)}(T_t) - \beta_{(1 \times 1)}(T_t) = 0.40 \text{ meV}/\text{\AA}^2$  using the estimated  $\Delta f^0$  and  $T_c - T_t = 6 \text{ K}$ . Williams *et al.* have reported that  $\beta_{(7 \times 7)}$  and  $\beta_{(1 \times 1)}$  are very close at  $T_c$  [20], which is consistent with our result. We should note, however, that the uncertainty of the  $T_t$ ,  $T_b$ , and  $T_c$  values estimated this way is at least  $1^\circ \text{C}$  and that the estimated  $f^0(T)$  and  $\beta(T)$  values can be markedly affected by this uncertainty.

At  $T_b > T > T_t$ , the  $(1 \times 1) \rightarrow (7 \times 7)$  phase transition occurs in the particular manner described earlier in this paper. The phase transition is usually on the side terrace lower than the  $(7 \times 7)$ -reconstructed terrace. This anisotropy is probably due to an anisotropic stress or a dc current induced effect. To determine which, we would have to observe the step rearrangement on a sample annealed without a dc current. We also confirmed the correlation of the  $(7 \times 7)$  reconstruction across a single-layer step. Goldberg *et al.* have pointed out that if an energetically preferred correlation is to occur, either lower-energy correlations must grow at the expense of higher-energy correlations or the  $(7 \times 7)$ -reconstructed terraces must nucleate and grow across the steps in a correlated manner [12]. The transient step bunching and the orderly phase transition on the terrace adjacent to the  $(7 \times 7)$ -reconstructed terrace is consistent with the latter mechanism and well explains the correlation of the  $(7 \times 7)$  reconstruction across a single-layer step.

In conclusion, HT-STM observations of the step rearrangement occurring during the  $(1 \times 1) \leftrightarrow (7 \times 7)$  transition on a vicinal Si(111) surface misoriented toward  $[\bar{1}\bar{1}2]$  show that new transient step bunching is due to the energy cost of forming  $(7 \times 7)$ -reconstructed step edges. We used our experimental result to estimate the differences in the surface energy of terraces and the free energy of individual steps caused by the  $(1 \times 1) \leftrightarrow (7 \times 7)$  phase transition. We also found the pathway by which the triple-layer steps on this surface are formed, and this pathway well explains the correlation of the  $(7 \times 7)$  recon-

struction across a single-layer step.

- [1] J. H. Neave, P. J. Dobson, B. A. Joyce, and J. Zhang, *Appl. Phys. Lett.* **47**, 100 (1985).
- [2] For example, J. M. Gaines, P. M. Petroff, H. Kroemer, R. J. Simes, R. S. Geels, and J. H. English, *J. Vac. Sci. Technol. B* **6**, 1378 (1988).
- [3] G. Wulff, *Z. Kristallogr. Mineral* **34**, 449 (1901).
- [4] R. J. Phaneuf and E. D. Williams, *Phys. Rev. Lett.* **58**, 2563 (1987).
- [5] R. J. Phaneuf, E. D. Williams, and N. C. Bartelt, *Phys. Rev. B* **38**, 1984 (1988).
- [6] R. J. Phaneuf and E. D. Williams, *Phys. Rev. B* **41**, 2991 (1990).
- [7] X.-S. Wang, J. L. Goldberg, N. C. Bartelt, T. L. Einstein, and E. D. Williams, *Phys. Rev. Lett.* **65**, 2430 (1990).
- [8] R. J. Phaneuf, N. C. Bartelt, E. D. Williams, W. Swięch, and E. Bauer, *Phys. Rev. Lett.* **67**, 2986 (1991).
- [9] M. Suzuki, Y. Homma, H. Hibino, T. Fukuda, T. Sato, M. Iwatsuki, K. Miki, and H. Tokumoto, *Jpn. J. Appl. Phys.* **32**, 3247 (1993).
- [10] H. Hibino, T. Fukuda, M. Suzuki, Y. Homma, T. Sato, M. Iwatsuki, K. Miki, and H. Tokumoto, *Phys. Rev. B* **47**, 13027 (1993).
- [11] N. C. Bartelt, T. L. Einstein, and C. Rottman, *Phys. Rev. Lett.* **66**, 961 (1991).
- [12] J. L. Goldberg, X.-S. Wang, J. Wei, N. C. Bartelt, and E. D. Williams, *J. Vac. Sci. Technol. A* **9**, 1868 (1991).
- [13] H. Hibino, Y. Homma, and T. Ogino (unpublished).
- [14] H. Tokumoto, K. Miki, and K. Kajiyama, *J. Cryst. Growth* **99**, 1329 (1990).
- [15] H. Hibino, Y. Kobayashi, Y. Shinoda, and K. Sugii, *Jpn. J. Appl. Phys.* **30**, 1337 (1991).
- [16] T. R. Ohno and E. D. Williams, *J. Vac. Sci. Technol. B* **8**, 874 (1990).
- [17] For example, Y. Homma, J. C. McClelland, and H. Hibino, *Jpn. J. Appl. Phys.* **29**, L2254 (1990).
- [18] N. C. Bartelt, E. D. Williams, R. J. Phaneuf, Y. Yang, and S. Das Sarma, *J. Vac. Sci. Technol. A* **7**, 1898 (1989).
- [19] J. Wei, X.-S. Wang, J. L. Goldberg, N. C. Bartelt, and E. D. Williams, *Phys. Rev. Lett.* **68**, 3885 (1992).
- [20] E. D. Williams, R. J. Phaneuf, J. Wei, N. C. Bartelt, and T. L. Einstein, *Surf. Sci.* **294**, 219 (1993).
- [21] For example, S. Hasegawa, Y. Nagai, T. Oonishi, and S. Ino, *Phys. Rev. B* **47**, 9903 (1993).
- [22] C. Alfonso, J. M. Bermond, J. C. Heyraud, and J. J. Métois, *Surf. Sci.* **262**, 371 (1992).
- [23] R. D. Meade and D. Vanderbilt, *Phys. Rev. B* **40**, 3905 (1989).
- [24] K. D. Brommer, M. Needels, B. E. Larson, and J. D. Joannopoulos, *Phys. Rev. Lett.* **68**, 1355 (1992).
- [25] H. Hibino and Y. Homma (unpublished).

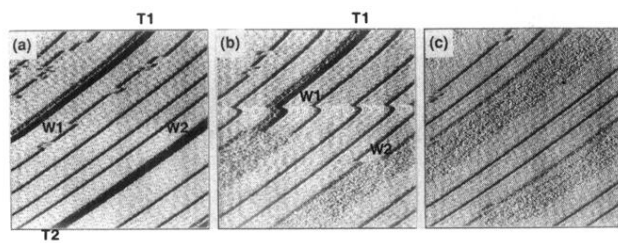


FIG. 1. Constant-height STM images of a vicinal Si(111) surface misoriented  $1.8^\circ$  toward  $[\bar{1}\bar{1}2]$ . Sample temperatures are (a)  $820^\circ\text{C}$ , (b) during heating, and (c)  $823^\circ\text{C}$ . (Scanning area:  $900 \times 900 \text{ \AA}$ . Sample bias: 2 V. Tunneling current: 0.2 nA.)

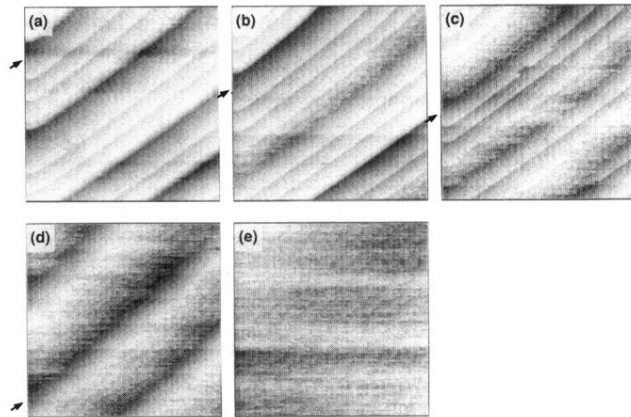


FIG. 2. Constant-current STM images of a vicinal Si(111) surface misoriented  $1.8^\circ$  toward  $[\bar{1}\bar{1}2]$ . Sample temperatures are (a)  $820^\circ\text{C}$ , (b)  $824^\circ\text{C}$ , (c)  $825^\circ\text{C}$ , (d)  $828^\circ\text{C}$ , and (e)  $830^\circ\text{C}$ . (Scanning area:  $1000 \times 100 \text{ \AA}$ . Sample bias: 2 V. Tunneling current: 0.2 nA.)

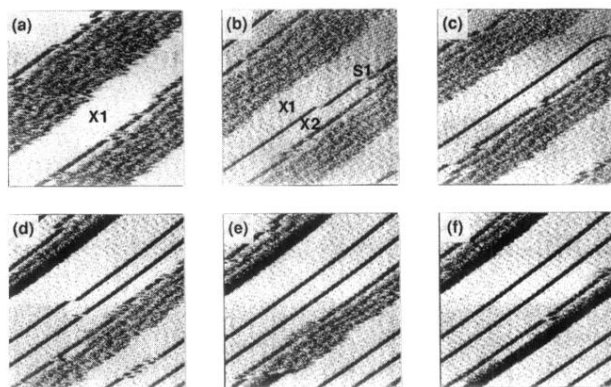
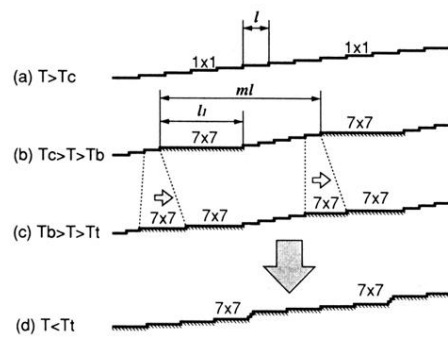


FIG. 3. Constant-height STM images taken while the sample temperature was decreased near  $825^{\circ}\text{C}$ . The images shown in (a)–(f) were taken at times 0, 35, 87.5, 122.5, 157.5, and 175 s. (Scanning area:  $750 \times 750 \text{ \AA}$ . Sample bias: 2 V. Tunneling current: 0.2 nA.)



**FIG. 4.** Schematic views of the temperature dependent step arrangement on a vicinal Si(111) surface misoriented  $1.8^\circ\text{C}$  toward  $[\bar{1}\bar{1}2]$ .